# Heat Transfer Modeling and Validation for Optically Thick Alumina Fibrous Insulation

**Kamran Daryabeigi**

## ABSTRACT

Combined radiation/conduction heat transfer through unbonded alumina fibrous insulation was modeled using the diffusion approximation for modeling the radiation component of heat transfer in the optically thick insulation. The validity of the heat transfer model was investigated by comparison to previously reported experimental effective thermal conductivity data over the insulation density range of 24 to 96 kg/m$^3$, with a pressure range of 0.001 to 750 torr (0.1 to 101.3 × 10$^3$ Pa), and test sample hot side temperature range of 530 to 1360 K. The model was further validated by comparison to thermal conductivity measurements using the transient step heating technique on an insulation sample at a density of 144 kg/m$^3$ over a pressure range of 0.001 to 760 torr, and temperature range of 290 to 1090 K.

## INTRODUCTION

Heat transfer through fibrous insulations has been the subject of great interest in the aerospace community for many years because of their use in thermal protection systems (TPS) for moderate to high temperature applications. The fibrous insulation systems used are either in bonded or unbonded form. The unbonded form consists of loose fibrous insulation mats typically used in blankets, while the bonded form is manufactured by sintering fibrous insulation mats to obtain a rigid insulation. The advanced flexible reusable surface insulation (AFRSI) blankets and reusable surface insulation tiles on the Space Shuttle Orbiter are examples of unbonded and bonded fibrous insulation. The focus of this paper is on an unbonded alumina fibrous insulation even though the basic heat transfer formulation applies to both bonded and unbounded insulations of various compositions.

Heat transfer through these high-porosity insulations is composed of combined radiation/conduction heat transfer. The conduction consists of both solid and gaseous conduction. In fibrous insulations with densities of 20 kg/m$^3$ or higher,

Kamran Daryabeigi, NASA Langley Research Center, MS 190, Hampton, VA 23681

natural convection is insignificant [1, 2]. Solid conduction is the least significant component of heat transfer for high-porosity, unbonded fibrous insulations. Solid conduction contribution increases with increasing insulation density. Radiation and gas conduction are the dominant modes of heat transfer. Radiation's significance increases with increasing temperature, and is inversely proportional to insulation density. The contribution of gas conduction increases with increasing temperature and static pressure, being negligible in vacuum conditions and increasing with increasing static pressure.

The standard practice for modeling heat transfer through fibrous insulations uses thermal conductivity measurements as a function of temperature and pressure obtained using either steady-state [3] or transient [4] techniques. The measured thermal conductivity lumps the contributions of the various modes of heat transfer without providing any insight into the physics or the contribution of the various heat transfer modes. The tabulated thermal conductivity data are then often used for analysis and design of TPS. One shortcoming of this technique is that the generated thermal conductivity data are applicable only to the specific composition used, and if some of the composition parameters such as density and fiber diameter change, a new set of data is needed. Furthermore, the thermal conductivities do not provide any insight into the relative contributions of various modes of heat transfer through the insulation, and therefore cannot be used for optimizing thermal performance of insulation.

Theoretical modeling of solid conduction through fibers and points of contact between them is difficult, therefore, various empirical and semi-empirical relations are used [5, 6]. Modeling of gas conduction in fibrous insulations requires knowledge of characteristic length (pore size), gas mean free path, and fiber orientation [5, 7]. Modeling of radiation heat transfer through fibrous insulations is more complicated, and has been the subject of various studies. A comprehensive review of various radiation models used for fibrous insulations is provided in Ref. [8]. The most accurate and comprehensive radiation modeling uses deterministic parameters that define the composition and morphology of the medium: distributions of fiber size and orientation, fiber volume fraction, and the spectral complex refractive index of fibers [9, 10]. This radiation modeling was used in a combined radiation/conduction heat transfer analysis and validated with experimental data on bonded and unbonded silica fibrous insulation samples [6], and further validated versus effective thermal conductivity data on unbonded silica fibrous insulation [11].

Radiation heat transfer through Saffil* alumina fibrous insulation had previously been modeled using the modified two-flux approximation with isotropic scattering [12], and with anisotropic scattering [2]. The higher-order radiation models had been developed for application to thin layers of low density alumina fibrous insulations located between thin reflective foils in high-temperature multilayer insulations [12, 13]. The thin low-density spacers had low optical thickness, therefore required modeling using higher-order radiation models such as the modified two-flux method. In the present study, the alumina fibrous insulation is modeled using the diffusion approximation for the radiation component of heat

* Thermal Ceramics Inc

transfer, which is valid for thicker insulation samples that are optically thick. The extinction coefficient needed for the radiation modeling is obtained using parameter estimation techniques in conjunction with previously obtained effective thermal conductivity data at a density of 24 kg/m$^3$ and pressure of 0.001 torr [2]. The resulting combined radiation/conduction heat transfer model is then validated versus effective thermal conductivity measurements for samples with densities between 24 and 96 kg/m$^3$ [2], and thermal conductivity measurements using the transient step heating technique [14] on a sample at a density of 144 kg/m$^3$ over a wide range of pressures and temperatures. The validated heat transfer model is then used to generate thermal conductivity data as a function of temperature and pressure at various insulation densities, which can then be used by thermal analysts for design and analysis of TPS.

## EXPERIMENTAL APPROACH

Data from two measurements techniques are used for validation of analytical heat transfer model. The measurement techniques, test conditions, test samples, and measurement uncertainties are briefly described.

### Effective Thermal Conductivity Measurements

Steady state effective thermal conductivity data had been previously generated in the NASA Langley Research Center's (LaRC) thermal-vacuum testing apparatus, described in detail elsewhere [15, 16]. The steady state test technique is used for measuring the effective thermal conductivity of a test sample with a large temperature difference maintained across the sample thickness, and is based on the American Society of Testing and Materials (ASTM) Standard C201 [17].

Tests were conducted with nominal sample hot side temperatures of 530, 690, 860, 1020, 1130, and 1250 K. At each hot side temperature set point, tests were conducted at nominal static pressures of 0.001, 0.01, 0.1, 0.5, 1, 5, 10, 100, and 750 torr in nitrogen gas. The average water-cooled plate temperature for the data was 297.3 ± 12.5 K. The fibrous insulation samples utilized randomly oriented alumina fibers with a mean effective fiber diameter of 4.5 x $10^{-6}$ m. Seven different fibrous insulation samples with various densities and thicknesses, presented in Table I, were tested. The samples had nominal densities of 24, 48, 72, and 96 kg/m$^3$, and sample thicknesses were 13.3, 26.6, and 39.9 mm. The samples had planar dimensions of 203 × 203 mm.

A detailed uncertainty analysis [18] was conducted in the present study for each measured quantity: hot and cold side temperatures, heat fluxes, and effective thermal conductivities. The overall uncertainty consisted of the contributions of random and bias uncertainties for each measured quantity, and uncertainties due to spatial non-uniformity of spatially-averaged quantities [19]. The average experimental uncertainty for data reported here was 6.1 ± 7.8%, with uncertainties varying between 1.1 and 36.3%. The highest uncertainties were at the lowest pressure and hot side temperature conditions (due to low signal to noise level

Table I . Listing of test samples used in effective thermal conductivity measurements.

| Sample thicknesses (mm) | Sample densities ($kg/m^3$) |
|---|---|
| 13.3 | 24.2, 48.6, 96.1 |
| 26.6 | 24.2, 48, 72 |
| 39.9 | 24.2, 72 |

associated with heat flux measurements at these low heat flux levels), and typically decreased with increasing pressure and hot side temperature.

### Thermal Conductivity Measurements

Thermal conductivity data were generated at a thermophysical properties laboratory using the transient step heating technique, described elsewhere [14], at temperatures of 286, 533, 811 and 1088 K, and pressures of 0.005, 1, and 760 torr in nitrogen gas. The fibrous insulation sample had a density of 144 $kg/m^3$, and was 49.5 mm in diameter and 6.6 mm thick. The reported uncertainty of these measurements was ±10%.

## ANALYTICAL APPROACH

In the absence of natural convection, the governing one-dimensional conservation of energy equation for the problem of combined radiation and conduction in a radiation participating media is given by

$$\rho c \frac{\partial T}{\partial t} = \frac{\partial}{\partial y}(k_c \frac{dT}{dy}) - \frac{\partial q_r}{\partial y} \tag{1}$$

where $\rho$ is density, $c$ is specific heat, $T$ is temperature, $t$ is time, $y$ is the spatial coordinate, $k_c$ is combined gas/solid thermal conductivity, and $q_r$ is radiant heat flux. If the insulation can be considered optically thick, then the diffusion approximation can be used with the radiant heat flux given by

$$q_r = -k_r \frac{dT}{dy} \tag{2}$$

where $k_r$ is the radiative thermal conductivity. Using this approximation the governing conservation of energy equation reduces to

$$\rho c \frac{\partial T}{\partial t} = \frac{\partial}{\partial y}(k \frac{dT}{dy}) \tag{3}$$

where k is obtained by superposition of the thermal conductivities due to solid conduction, gas conduction, and radiation

$$k = k_s + k_g + k_r \tag{4}$$

where $k_s$ and $k_g$ are the solid and gas conduction thermal conductivities.

The formulation for each of the thermal conductivity terms in Eq. 4 is provided. The radiant thermal conductivity is

$$k_r = \frac{16\sigma n^2 T^3}{3\rho e} \tag{5}$$

where $\sigma$ is the Stefan-Boltzmann constant, $n$ is the index of refraction, and $e$ is the specific extinction coefficient of the fiber medium. The optical thickness, $\tau$, is provided by

$$\tau = \rho e L \tag{6}$$

where $L$ is the insulation thickness. Insulation can be considered optically thick only if $\tau >> 1$, which is valid for insulation samples used in this study with optical thicknesses varying between 16 and 500. The index of refraction in fibrous media is a strong function of fiber volume fraction ($f_v$) and weak function of temperature [20]. The temperature dependence of the index of refraction was neglected and a linear curve fit of the effective index of refraction with fiber volume fraction was used, with the effective index of refraction increasing with increasing fiber volume fraction. The specific extinction coefficient for this fibrous insulation was unknown, and had to be estimated from the experimental data. It was assumed that the specific extinction coefficient had a third order polynomial dependence on temperature, with the polynomial coefficients obtained from a parameter estimation technique in conjunction with experimental effective thermal conductivity data.

An empirical model was used to model solid conduction thermal conductivity of fibrous insulation [5]

$$k_s(T) = f_v^3 k_s^*(T) \tag{7}$$

which relates the solid thermal conductivity of fibrous insulation to the thermal conductivity of bulk fiber material, $k_s^*$, and fiber volume fraction, $f_v$.

Gas thermal conductivity does not vary with pressure but the exchange of heat from gas molecules to bounding solid surfaces is influenced by the environmental pressure in the rarefied and transition flow transport regimes. Thus, an effective gas thermal conductivity was defined as [7]

$$k_g(T,P) = \frac{k_{g0}(T)}{\Phi + 2\Psi \frac{\beta}{\mathrm{Pr}} Kn} \tag{8}$$

where $k_{g0}(T)$ is the thermal conductivity of the gas, and $Pr$ is the Prandtl number. The parameter $\beta$ is defined as

$$\beta = \left(\frac{2-\alpha}{\alpha}\right)\frac{2\gamma}{(\gamma+1)} \tag{9}$$

with $\alpha$ being the thermal accommodation coefficient, and $\gamma$ being the ratio of specific heats at constant volume and pressure. $Kn$ is the Knudsen number, provided by

$$Kn = \frac{\lambda}{L_c} \tag{10}$$

The gas mean free path, $\lambda$, is

$$\lambda = \frac{K_B T}{\sqrt{2}\pi d_m^2 P} \tag{11}$$

where $K_B$ is the Boltzmann constant, $d_m$ is the gas collision diameter, and $P$ is the pressure. An empirical formulation for gas conduction characteristic length (pore size), $L_c$, is used [5]

$$L_c = \frac{\pi}{4}\frac{d_p}{f_v} \tag{12}$$

where $d_p$ is the fiber mean diameter. The parameters $\Phi$ and $\Psi$ depend on the Knudsen number. $\Phi = 1$, $\Psi = 0$ for Knudsen number less than 0.01 (continuum regime), $\Phi = 1$, $\Psi = 1$ for Knudsen number between 0.01 and 10 (transition regime), and $\Phi = 0$, $\Psi = 1$ for Knudsen number greater than 10 (free-molecular regime). The thermal accommodation coefficient was assumed to be unity, while the ratio of specific heats at constant volume and pressure was assumed to be 1.4.

The analytical thermal conductivity in Eq. (4) is obtained by substituting for radiant, solid, and gas thermal conductivity terms from Eqs. 5, 7, and 8, respectively. The analytical prediction is then directly compared with transient step heating thermal conductivity measurements. For comparison with effective thermal conductivity measurements, the analytical thermal conductivity had to be numerically integrated with respect to temperature between the experimental hot and cold side temperatures, $T_H$ and $T_C$

$$k_e = \frac{1}{T_H - T_C}\int_{T_C}^{T_H} k\partial T \tag{13}$$

## DISCUSSION OF RESULTS

A genetic-algorithm based parameter estimation technique [21] was used to obtain the unknown coefficients of the third order polynomial fit for the specific extinction coefficient. Data for an insulation sample at a density of 24 kg/m$^3$ and thicknesses of 13.3, 26.6 and 39.9 mm at 0.001 torr pressure were used for the parameter estimation. At this pressure, gas conduction is negligible, and at this low fibrous insulation density the ratio of radiation to solid conduction is highest, thus providing the highest sensitivity for obtaining accurate estimates of the radiation specific extinction coefficient. The parameter estimation was accomplished by minimizing the sum of the square of differences between measured and predicted effective thermal conductivities. The predicted effective thermal conductivities were obtained by using various estimates of unknown parameters to calculate radiant thermal conductivity based on Eq. (5), calculating the thermal conductivity according to Eq. (4), and then calculating the effective thermal conductivity based on Eq. (13). The variation of best estimate specific extinction coefficient with

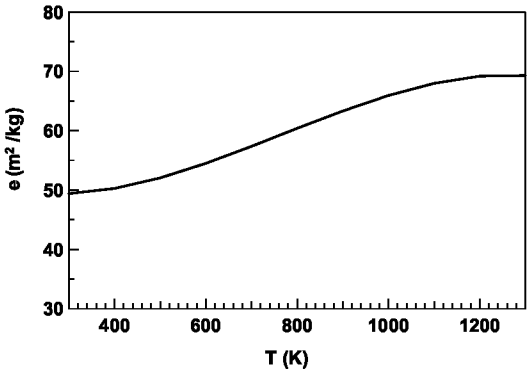


Figure 1. Variation of best fit specific extinction coefficient with temperature.

temperature is shown in Figure 1. The comparison of measured and predicted effective thermal conductivities for sample density of 24 kg/m$^3$ at 0.001 torr pressure as a function of hot side temperature is shown in Figure 2a. The line represents the analytical prediction, while the symbols represent experimental data. The calculated experimental uncertainties are also shown in the figure. The rms deviation between measurements and predictions for data at this density was 5.1%. To evaluate how good the radiation and conduction components of heat transfer have been modeled, the comparison of measured and predicted effective thermal conductivities at sample densities of 48, 72 and 96 kg/m$^3$ at 0.001 torr pressure as a function of hot side temperature is shown in Figure 2b. The rms deviations between measured and predicted effective thermal conductivities were 3.1, 7.1, and 0.9%, for data at sample densities of 48, 72 and 96 kg/m$^3$, respectively. These rms deviations were typically within the experimental uncertainties. The close agreement of predictions and measurements of effective thermal conductivity at 0.001 torr indicate that the radiation and solid conduction components of heat transfer through this alumina fibrous insulation at various densities has been modeled satisfactorily.

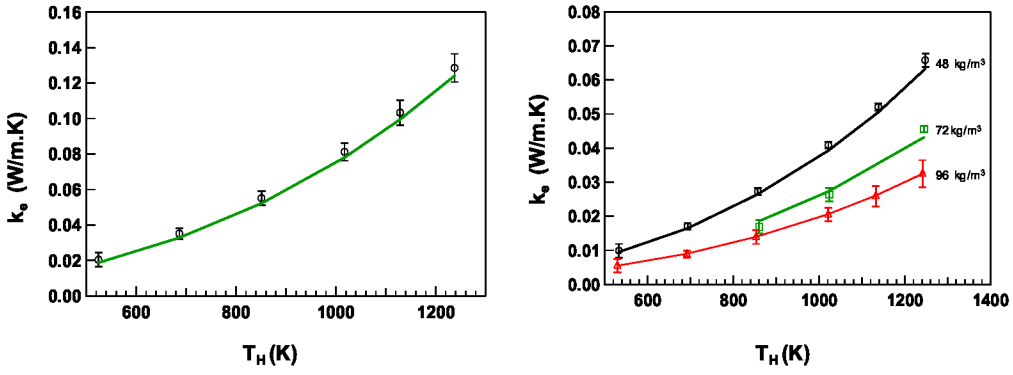


Figure 2. Variation of predicted and measured effective thermal conductivity with hot side temperature at 0.001 torr at densities of: a) 24 kg/m$^3$ b) 48, 72 and 96 kg/m$^3$.

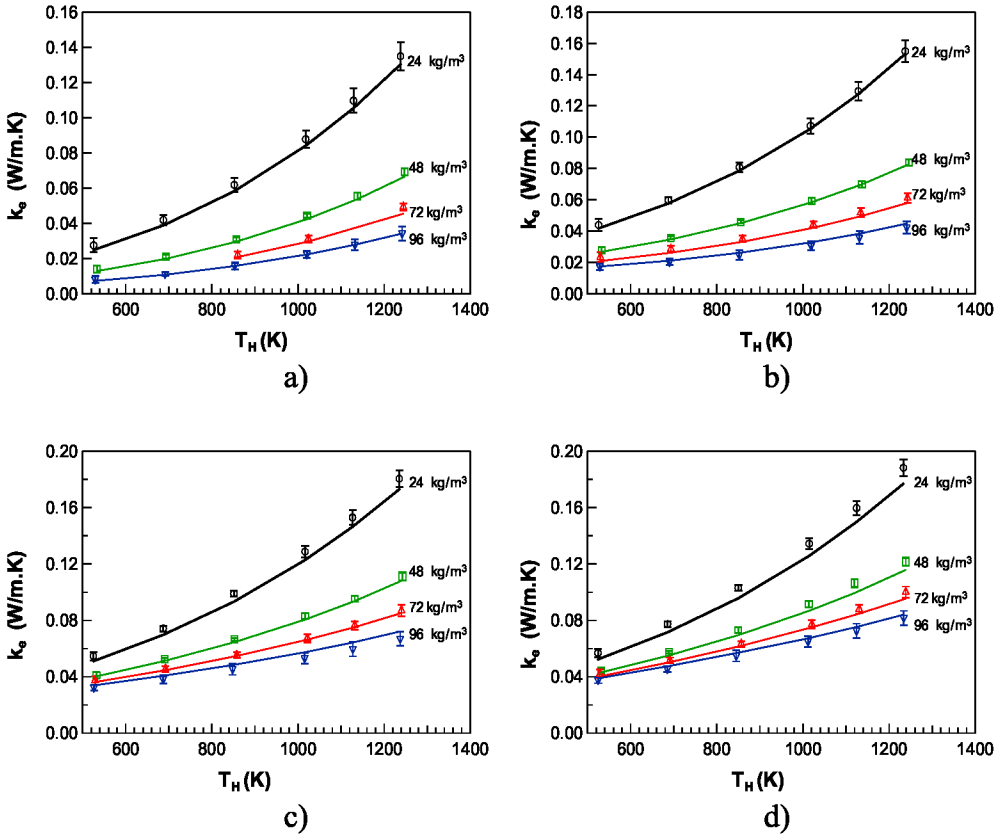


Figure 3. Variation of predicted and measured effective thermal conductivity with hot side temperature at various insulation densities at static pressures of: a) 0.1 torr b) 1 torr c) 10 torr d) 100 torr.

Once the radiation and solid conduction components have been modeled correctly, all that is needed is to add the contribution of gas conduction, from Eq. (8), to calculate thermal conductivity at higher pressures. Comparisons of predicted and measured effective thermal conductivities at pressures of 0.1, 1, 10, and 100 torr for sample densities of 24, 48, 72 and 96 kg/m$^3$ as a function of hot side temperature are shown in Figure 3a-d. There was good agreement between measured and predicted effective thermal conductivities at these higher pressures as seen in the figures, with predictions typically matching measurements to within the experimental uncertainties. At 100 torr, even though the agreement at densities of 24 and 48 kg/m$^3$ was outside the reported experimental uncertainties, the differences between predictions and measurements were between 6 and 8% for the 24 kg/m$^3$ data, and between 3 and 6% for the 48 kg/m$^3$ data. The rms deviations between measurements and predictions for data over all pressures and temperatures for sample densities of 24, 48, 72 and 96 kg/m$^3$ were 5.6, 6.1, 8.6, and 3.8%, respectively, with an overall rms deviation of 6.3% for data at all densities.

The variation of measured and predicted effective thermal conductivity with static pressure for sample density of 48 kg/m$^3$ at hot side temperatures of 860 and 1250 K is shown in Figure 4. The overall agreement is good with rms deviations of

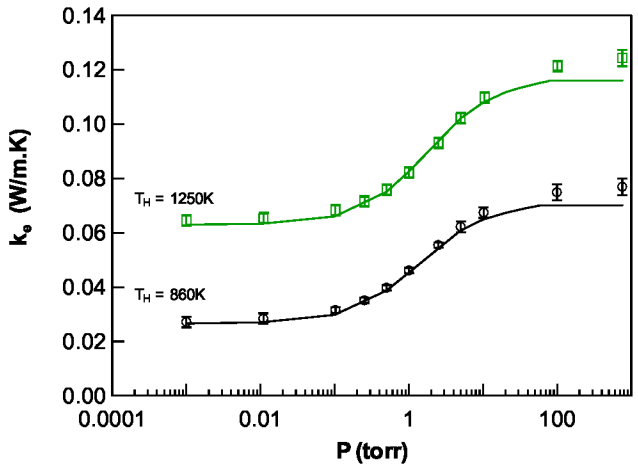


Figure 4. Variation of predicted and measured effective thermal conductivity with pressure for sample density of 48 kg/m$^3$ at hot side temperatures of 860 and 1250 K.

3.2 and 4.7% for data at 860 and 1250 K, respectively. Even though the predictions at pressures of 100 torr and higher are not within the uncertainty range of experimental data, the difference between predictions and measurements at these pressures had an average of 6.9%, which was a very reasonable agreement.

The analytical model was then compared to thermal conductivity measurements using the transient step heating technique. Comparison of predicted and measured thermal conductivities as a function temperature for tests at three test pressures is shown in Figure 5. The predictions matched the experimental data within the experimental uncertainty range, further validating the analytical model.

With the validated heat transfer model for the alumina fibrous insulation, thermal conductivity predictions as a function of temperature and pressure for various densities can then be generated for use by thermal analysts who can only use tabulated thermal conductivity data in their thermal analysis software packages. Variation of thermal conductivity with temperature at various static pressures for insulation densities of 48 and 96 in air are shown in Figure 6.

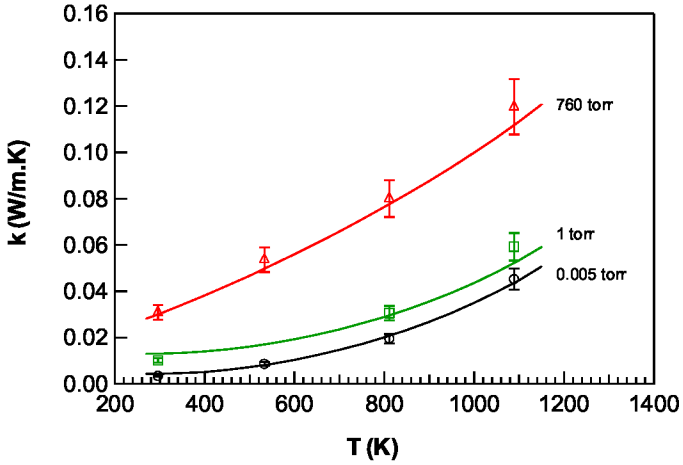


Figure 5. Variation of predicted and measured thermal conductivity with temperature at various pressures for sample density of 144 kg/m$^3$.

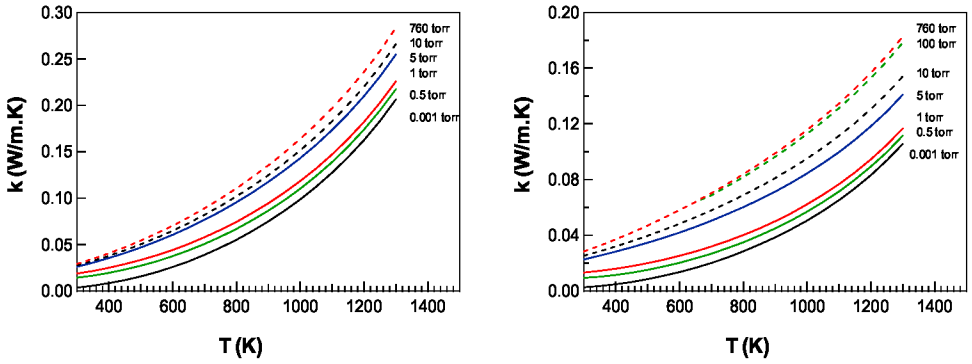


a) b)

Figure 6. Variation of predicted analytical thermal conductivity with temperature at various pressures for sample densities of: a) 48 kg/m$^3$, b) 96 kg/m$^3$.

The use of the physics based heat transfer model presented in this study has certain advantages compared to using tabulated thermal conductivity values. Once the specific required parameters are known (fiber diameter, specific extinction coefficient and index of refraction), the model can be applied to samples at various densities. Furthermore, data can be generated for various gaseous media if the gas collision diameter and variations of gas thermal conductivity and Prandtl number with temperature are known. The most accurate model can be obtained by using deterministic parameters that define the composition and morphology of the medium: distributions of fiber size and orientation, fiber volume fractions, and the spectral complex refractive index of the fibers [6, 11]. If all the desired deterministic parameters are not known, experimental thermal conductivity data and parameter estimation techniques can be utilized to infer relevant parameters needed for satisfactory modeling of combined radiation/conduction heat transfer in fibrous insulations.

## CONCLUDING REMARKS

Combined radiation/conduction heat transfer through unbonded alumina fibrous insulation was modeled using the diffusion approximation for modeling the radiation component of heat transfer. The specific extinction coefficient was determined using parameter estimation techniques applied to existing experimental steady-state effective thermal conductivity data. The validity of the heat transfer model was investigated by comparison with experimental effective thermal conductivity data over the density range of 24 to 96 kg/m$^3$, pressure range of 0.001 to 750 torr, and test specimen hot side temperature range of 530 to 1360 K. The rms deviation between predicted and measured effective thermal conductivities for the range of pressures, temperatures, and densities tested was 6.3%. The model was further validated by thermal conductivity measurements using the transient step heating technique on an insulation sample at a density of 144 kg/m$^3$, over a pressure range of 0.001 to 760 torr, and temperature range of 290 to 1090 K. The close agreement between measured and predicted thermal conductivities further validated

the analytical model. The validated heat transfer model for the alumina fibrous insulation was then used to generate thermal conductivity predictions as a function of temperature and pressure for various densities for use by thermal analysts for design and analysis of TPS.

## ACKNOWLEDGEMENTS

The author wishes to express his gratitude to the following individuals for their significant contributions to this work: George R. Cunnington, Cunnington and Associates, for providing extremely invaluable insights in thermal modeling and testing of insulations; Jeffrey R. Knutson, NASA Langley Research Center, for conducting effective thermal conductivity measurements; and Jozef Gembarovic, TPRL Inc, for providing thermal conductivity measurements.

## REFERENCES

1. Stark, C., and Fricke, J., "Improved Heat-Transfer Models for Fibrous Insulations," *International Journal of Heat and Mass Transfer*, Vol. 36, No. 3, 1993, pp. 617-625.
2. Daryabeigi, K., "Heat Transfer in High-Temperature Fibrous Insulation," *Journal of Thermophysics and Heat Transfer*, Vol. 17, No. 1, pp. 10-20, 2003.
3. Banas, R.P, and Cunnington, G. R., "Determination of Effective Thermal Conductivity for the Space Shuttle Orbiter's Reusable Surface Insulation," AIAA 74-730, July 1974.
4. Williams, S. D., and Curry, D. M., "Predictions of Rigid Silica Based Insulation Conductivity," NASA TP-3276, January 1993.
5. Verschoor, J. D., and Greebler, P., and Manville, N.J., "Heat Transfer by Gas Conduction and Radiation in Fibrous Insulations," *Transactions of the Society of Mechanical Engineers*, Vol. 74, No. 8, 1952, pp. 961-968.
6. Lee, S. C., and Cunnington, G. R., "Conduction and Radiation Heat Transfer in High-Porosity Fiber Thermal Insulation," *Journal of Thermophysics and Heat Transfer*, Vol. 14, No. 2, 2000, pp. 121-136.
7. Gebhart, B., *Heat Conduction and Mass Diffusion*, McGraw-Hill, New York, 1993, pp. 442-444.
8. Lee, S. C., and Cunnington, G. R, "Theoretical Models for Radiative Transfer in Fibrous Media," *Annual Review in Heat Transfer*, Ed. by C. L. Tien, Vol. 9, Begell House, NY, 1998, pp. 159-212.
9. Lee, S. C., "Radiative Transfer Through a Fibrous Medium: Allowance for Fiber Orientation," *Journal of Quantitative Spectroscopy and Radiative Transfer*, Vol. 36, No. 3, 1986, pp. 253-263.
10. Lee, S. C., "Scattering Phase Function for Fibrous Materials," *International Journal of Heat and Mass Transfer*, Vol. 33, No. 10, 1990, pp. 2183-2190.
11. Daryabeigi, K., Cunnington, G. R., and Knutson, J. R., "Measurement of Heat Transfer in Unbonded Silica Fibrous Insulation and Comparison with Theory," *Thermal Conductivity*, Ed. by J.R. Koenig and H. Ban, Vol. 29, DEStech Publications Inc., Lancaster, PA, 2008, pp. 292-301.
12. Daryabeigi, K., "Thermal Analysis and Design Optimization of Multilayer Insulation for Reentry Aerodynamic Heating," *Journal of Spacecraft and Rockets*, Vol. 39, No. 4, 2002, pp. 509-514.

13. Daryabeigi, K., Miller, S. D., and Cunnington, G. R., "Heat Transfer in High-Temperature Multilayer Insulations," Proceedings of the 5th European Workshop on Thermal Protections Systems and Hot Structures, ESTEC, Noordwijk, the Netherlands, May 17-19, 2006.

14. Gembarovic, J., and Taylor, R. E, "A Method for Thermal Diffusivity Determination of Thermal Insulators," *International Journal of Thermophysics*, Vol. 28, No. 6, Dec 2007, pp. 2164-2175.

15. Daryabeigi, K., "Effective Thermal Conductivity of High Temperature Insulations for Reusable Launch Vehicles," NASA TM-1999-208972, February 1999.

16. Daryabeigi, K., "Analysis and Testing of High Temperature Fibrous Insulation for Reusable Launch Vehicles," AIAA Paper 99-1044, January 1999.

17. Standard Test Method for Thermal Conductivity of Refractories, *Annual Book of ASTM Standards,* Vol. 15.01, American Society for Testing and Materials, West Conshohocken, PA, pp. 54-59, 2000.

18. Coleman, H. W., and Steele, W. G., *Experimentation and Uncertainty Analysis for Engineers*, Wiley, New York, 1989.

19. Sullins, A. D., "Heat Transfer in High Porosity Open Cell Nickel Foam," M.S. Thesis, School of Engineering and Applied Sciences, The George Washington University, August 2001.

20. Caren, R. P., "Radiation Transfer from Metal to a Finely Divided Particulate Medium", *Jour Heat Transfer,* No. 154, 1969, pp. 154-156.

21. Haupt, R. L., and Haupt, S. E., *Practical Genetic Algorithms,* Wiley, New York, 1998.